Earth and Planetary Science Letters 463 (2017) 118–126

Contents lists available at ScienceDirect

Earth and Planetary Science Letters

www.elsevier.com/locate/epsl

Rapid deglacial injection of nutrients into the tropical Atlantic via Antarctic Intermediate Water

David-Willem Poggemann [a,*], Ed C. Hathorne [a], Dirk Nürnberg [a], Martin Frank [a], Imke Bruhn [a], Stefan Reißig [a], André Bahr [b]

[a] *GEOMAR Helmholtz Centre for Ocean Research Kiel, D-24148 Kiel, Germany*
[b] *Heidelberg University, Institute of Earth Science, D-69120 Heidelberg, Germany*

A R T I C L E   I N F O

Article history:
Received 24 March 2016
Received in revised form 16 January 2017
Accepted 25 January 2017
Available online xxxx
Editor: H. Stoll

Keywords:
Atlantic intermediate water circulation
Caribbean nutrient concentrations
Cd reconstruction
Atlantic Meridional Overturning circulation
Antarctic Intermediate Water
deglacial CO_2

A B S T R A C T

As part of the return flow of the Atlantic overturning circulation, Antarctic Intermediate Water (AAIW) redistributes heat, salt, CO_2 and nutrients from the Southern Ocean to the tropical Atlantic and thus plays a key role in ocean–atmosphere exchange. It feeds (sub)tropical upwelling linking high and low latitude ocean biogeochemistry but the dynamics of AAIW during the last deglaciation remain poorly constrained. We present new multi-decadal benthic foraminiferal Cd/Ca and stable carbon isotope (δ^{13}C) records from tropical W-Atlantic sediment cores indicating abrupt deglacial nutrient enrichment of AAIW as a consequence of enhanced deglacial Southern Ocean upwelling intensity. This is the first clear evidence from the intermediate depth tropical W-Atlantic that the deglacial reconnection of shallow and deep Atlantic overturning cells effectively altered the AAIW nutrient budget and its geochemical signature. The rapid nutrient injection via AAIW likely fed temporary low latitude productivity, thereby dampening the deglacial rise of atmospheric CO_2.

1. Introduction

The Atlantic Meridional Overturning Circulation (AMOC) today is driven by the deep water formation in the N-Atlantic (e.g. Talley, 2013) and underwent considerable changes during the transition from the Last Glacial Maximum (LGM) to the Holocene (McManus et al., 2004; Gherardi et al., 2009; Böhm et al., 2015). During abrupt deglacial climate cooling periods, namely the Heinrich Stadial 1 (HS1, 18–14.6 ka, thousand years) and the Younger Dryas (YD, 12.8–11.5 ka), a severe weakening or even collapse of the AMOC occurred. As a consequence, the temperature contrast between the hemispheres decreased, the Southern Ocean (SO) warmed and sea ice retreated (Toggweiler and Lea, 2010). Amplified by the synchronous strengthening and southward shift of the trade winds and the westerly wind belt, upwelling of nutrient-rich intermediate to deep water masses in the E-Atlantic and in the SO resumed after these cold periods (e.g. Broecker, 1998; Anderson et al., 2009; Bradtmiller et al., 2016). As the deep stratification in the SO, which likely characterised the LGM, collapsed (Burke and Robinson, 2012), outgassing from upwelling abyssal water released CO_2 to the atmosphere (e.g. Denton et al., 2010; Jaccard et al., 2016). A synchronous re-organisation of intermediate to deep Atlantic ocean water mass exchange likely enhanced these processes: The apparently weakened or even ceased formation of southward flowing shoaled North Atlantic Deep Water (NADW), termed Glacial North Atlantic Intermediate Water (GNAIW), influenced the oceanic circulation Atlantic-wide and likely contributed to the enhanced upwelling and release of CO_2 in the SO (e.g. Broecker, 1998; Burke and Robinson, 2012). Other studies have suggested changes in NADW formation as a major driving factor for the deglacial atmospheric CO_2 increase (e.g. Hain et al., 2014; Lund et al., 2015). In addition, the southward shift of the westerly wind belt led to a decrease in dust supply and therefore lower iron fertilisation of surface waters in the SO (Jaccard et al., 2016).

The implications of these deglacial atmospheric and oceanographic perturbations during HS1 and/or the YD for Atlantic intermediate water circulation, in particular for AAIW and GNAIW, are contentious. A weakened southward flow of northern sourced waters has been hypothesised to have resulted in an extended northward expansion of AAIW into the NW-Atlantic (e.g. Pahnke et al., 2008; Hendry et al., 2012) or even further north (Rickaby and Elderfield, 2005). In contrast, other studies have either suggested a continuous or even enhanced advection of northern sourced wa-

* Corresponding author.
E-mail address: dpoggemann@geomar.de (D.-W. Poggemann).

http://dx.doi.org/10.1016/j.epsl.2017.01.030

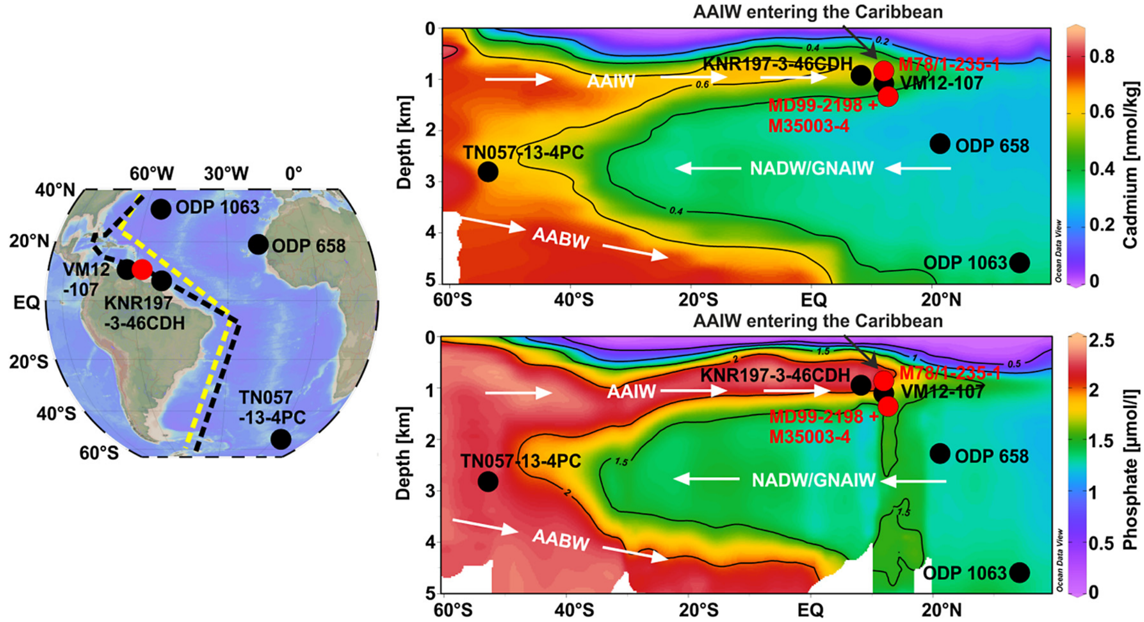

Fig. 1. Location of study sites, cadmium and phosphate concentration of different Atlantic water masses: *Left:* Bathymetric chart of the Atlantic Ocean with locations of the sediment cores studied here (red dot, identifiers in the right side profiles). Reference records of previous studies are depicted by black dots (Böhm et al., 2015; McManus et al., 2004 (ODP 1063); Meckler et al., 2013 (ODP 658); Xie et al., 2014 (VM12-107); Huang et al., 2014 (KNR197-3-46CDH); Anderson et al., 2009 (TN057-13-4PC)). Dashed lines show cadmium and phosphate sections (yellow = Cd; black = P). *Right:* S–N-trending cadmium- (top, data from GEOTRACES; Mawji et al., 2015) and phosphate-profile (bottom, data from WOA; Boyer et al., 2013) with locations of proxy records, placed at the according water depths. Major Atlantic water masses can be differentiated by their phosphate and cadmium concentrations (AAIW = Antarctic Intermediate Water; NADW = North Atlantic Deepwater; GNAIW = Glacial North Atlantic Intermediate Water; AABW = Antarctic Bottom Water). Figures were created using Ocean Data View (Schlitzer, 2015). (For interpretation of the references to colour in this figure legend, the reader is referred to the web version of this article.)

ters at intermediate depth (Came et al., 2003, 2008; Xie et al., 2012) that may even have resulted in the absence of AAIW during these periods (Huang et al., 2014; Howe et al., 2016). Recent data also indicate that northern sourced waters continuously influenced mid-depth waters in the SW-Atlantic and that the AMOC may not have collapsed completely (e.g. Lund et al., 2015). At the same time a postulated short-term breakdown of SO stratification may have led to increased AAIW ventilation during northern hemisphere cooling events (Burke and Robinson, 2012).

To reconstruct past changes in intermediate and deep Atlantic circulation patterns benthic foraminiferal Cd/Ca has been used routinely as a proxy for seawater cadmium concentrations. Seawater cadmium concentrations (Cd_W) are closely correlated with phosphate concentrations. Prior work has demonstrated that benthic foraminifera incorporate Cd as a function of Cd_W. Hence, the Cd content of fossil calcitic tests reflects the distinct nutrient concentrations of bottom water masses in the past (Boyle, 1988, 1992). Various studies have demonstrated the reliability of benthic foraminiferal Cd/Ca ratios to reconstruct deep and intermediate water masses in the past (e.g. Came et al., 2003; Rickaby and Elderfield, 2005; Came et al., 2008; Bryan and Marchitto, 2010).

Our study reconstructs the deglacial intermediate water mass changes in the tropical W-Atlantic based on a unique sediment core from Tobago Basin presently bathed by the tip of the AAIW tongue (M78/1-235-1, 852 m) (Fig. 1). We also studied adjacent but deeper core MD99-2198 located at the modern lower boundary of AAIW. Complemented by published Cd/Ca data of core M35003 (Zahn and Stüber, 2002; same location and depth as MD99-2198), the composite Cd/Ca dataset from ∼1300 m adds information on past changes in the vertical extent of AAIW (Fig. 1). Our benthic foraminiferal Cd/Ca (endobenthic species *Uvigerina spp.*) are complemented by $\delta^{13}C$ time series (epibenthic species *Cibicidoides pachyderma*) and allow intermediate nutrient inventory and circulation changes to be deciphered at unprecedented temporal resolution for the past ∼24,000 years.

2. Material and methods

We analysed the sediment cores M78/1-235-1 (11°36.53′N, 60°57.86′W, 852 m) and MD99-2198 (12°05.51′N, 61°14.01′W, 1330 m) (Fig. 1), both from the Tobago Basin, to reconstruct the Cd_W and $\delta^{13}C$ signatures of past bottom waters for the time interval from ∼24 ka BP to late Holocene. Today, sediment core M78/1-235-1 is bathed by AAIW located at a depth between ∼600 and 1200 m in the S-Caribbean. Core MD99-2198 is located nearby but at greater depth at the transition zone between AAIW and NADW. Together, the proxy data obtained from these sediment cores should reveal vertical and frontal movements of AAIW and NADW/GNAIW. Sediment core MD99-2198 was sampled at 5 cm-intervals and at a slightly lower resolution during the Holocene. Core M78/1-235-1 was sampled at 2 cm-intervals. For the YD and HS1 intervals both cores were sampled at 1 cm-resolution to monitor rapid changes in Cd_W at the highest resolution possible. Samples were freeze-dried before wet sieving.

2.1. Age models

The age model for sediment core M78/1-235-1 was generated by linear interpolation between 9 Accelerator Mass Spectrometer AMS ^{14}C dates (see supplementary Table S1, Fig. S1), of which 4 dates are published (Hoffmann et al., 2014). AMS ^{14}C measurements were carried out at the Cologne AMS (Cologne, Germany) and Beta Analytic Limited (London, UK). Mixed layer dwelling *Globigerinoides ruber* and *Globigerinoides sacculifer* were used (with the exception of one sample where some *Orbulina universa* were included to ensure a sufficient sample mass) and calibrated with CALIB 7.1 using the MARINE13 reservoir age data set (Reimer et al., 2013). The average sedimentation rate is ∼18 cm/kyr. For sediment core MD99-2198 we used the established, previously published age model (Pahnke et al., 2008).

2.2. Cd/Ca measurements

A minimum of 10 tests of the endobenthic foraminiferal species *Uvigerina spp.* (315–400 µm size fraction), the most abundant benthic species in sediment cores M78/1-235-1 and MD99-2198, were cleaned with reductive and oxidative reagents following established techniques (Boyle and Rosenthal, 1996; Rosenthal et al., 1997). Several studies showed that the endobenthic species *Uvigerina spp.* can be used to reliably reconstruct Cd_W of ancient water masses (e.g. Boyle, 1988; Zahn and Stüber, 2002; Bryan and Marchitto, 2010). To improve the efficiency of the Cd/Ca analyses, a novel technique using an Elemental Scientific "seaFAST" pre-concentration system coupled to an Agilent 7500ce ICP-MS was adapted from a method for seawater trace metal analyses (Hathorne et al., 2012). This method is well suited for small sample sizes as all the Cd contained in the 2.5 ml sample loop and loaded onto the preconcentration column is measured during time resolved analysis of the elution peak. While the Cd and other trace metals are loaded onto the column the Ca matrix is removed allowing high Ca concentration solutions to be measured with minimal instrumental drift. Therefore, in a first step an aliquot of the dissolved sample was diluted, scandium added as an internal standard, and the Ca concentration determined using conventional nebulisation. Then for the Cd analyses, all samples were diluted to exact Ca-concentrations, which ranged from 10 to 100 ppm Ca depending on sample size. Indium was added to every sample at a concentration of 100 parts per trillion (ppt), to check for any drift or changes in preconcentration efficiency, and was routinely within 5% of the initial In intensity throughout the run. Similar column yields were obtained for Cd and In and the yield for Cd in sample matrix measured online was 94%. The column yield was reproducible and linear as evident from calibration curves obtained ($r^2 > 0.99$) over a range of Cd concentrations (1–40 ppt). Measuring ^{111}Cd no interferences were observed and detection limits (defined as 3.3 times the standard deviation of blank measurements) of around 0.6 ppt were obtained. All blanks, calibration standards and reference materials, with the same Ca concentration as the samples, were run through the preconcentration column exactly like the samples.

To assess accuracy and allow comparison with subsequent studies the Cd/Ca ratio of the limestone powder reference material ECRM-752 (Greaves et al., 2008; dissolved in weak nitric acid and centrifuged as recommended for Mg/Ca analyses) was measured ($n = 20$) and the mean during the course of this study found to be 562 ± 22 nmol/mol. This is in good agreement with the average values of two other laboratories (544 ± 18 nmol/mol and 574 ± 13 nmol/mol, respectively; Greaves et al., 2008). This Cd/Ca value is an order of magnitude higher than that found in our intermediate water depth samples so for routine quality control the ECRM-752 solution was diluted by a factor of 10 using a Ca single element solution to have the same Ca concentration as samples. The single element Ca solution was also run as a blank and found to contain no measurable Cd signal. The reproducibility is dependent on the sample size, with larger samples having better precision (e.g. 3% at 50 ppm Ca, 5.6% at 25 ppm Ca and 6.6% at 10 ppm Ca), but was always better than 15% (2σ). Three samples with sufficient material were used to perform replicate measurements. The average standard deviation of these replicates (8.91 nmol/mol, 2σ) equates to an uncertainty of the Cd_W data of 0.076 nmol/kg using the published depth dependent calibration of Boyle (1992). This estimate does not include uncertainties in the apparent partition coefficient (see Marchitto and Broecker, 2006, and Bryan and Marchitto, 2010 for a thorough discussion of this) but using a D_{Cd} of 1.3 for core M78/1-235-1 and of 1.46 for core MD99-2198 we obtain Cd_W values for the youngest Holocene samples that match modern Cd concentrations in the W-Atlantic (GEOTRACES; Mawji et al., 2015). Using a partition coefficient of 1.7 suggested by Bryan and Marchitto (2010), based on an assumed $Cd:PO_4$ relationship, leads to Cd_W values 0.15 nmol/kg lower than observed near the core sites.

2.3. Composite Cd_W-record for 1300 m water depth

In order to support previously published Cd_W-data from the modern transition zone between modern AAIW and NADW in the tropical W-Atlantic (Zahn and Stüber, 2002; core M35003), we produced a new higher resolution Cd_W record from the same location and water depth (core MD99-2198). The age model of the latter sediment core is based on AMS ^{14}C dates and optical tuning of δ^{13}C records of both cores (Pahnke et al., 2008). As both Cd_W records should have the same age intervals, we created a composite Cd_W-record by simple merging, which enables the elimination of high frequency noise (Fig. 2B).

2.4. δ^{13}C measurements

For δ^{13}C analyses we used 3–5 tests of the epibenthic species *Cibicidoides pachyderma* per sample. This benthic species is considered to record the seawater δ^{13}C signature most reliably (e.g. Duplessy et al., 1984; Zahn et al., 1986; Curry and Oppo, 2005; Marchitto and Broecker, 2006). The uncleaned samples were measured using a Thermo Fischer Scientific MAT 253, equipped with an automated CARBO Kiel IV carbon preparation device. Stable isotope measurements are referenced to the "NBS 19" (National Bureau of Standards) carbonate standard and the "Standard Bremen" (in-house standard). The results are reported against the VPDB scale (Vienne Pee Dee Belemnite). The analytical error was $\pm 0.05‰$ (2σ, $n = 16$) and the long-term reproducibility $\pm 0.035‰$ (2σ, $n = 172$), based on repeated standard measurements.

2.5. Data outliers

Within the high resolution data a small number of single data points appear unrealistically high compared with the surrounding data (Fig. 2). Therefore a Grubb's test was performed and one Cd_W and two δ^{13}C data points from core M78/1-235-1 and three Cd_W data points published from core M35003 (Zahn and Stüber, 2002) were rejected as outliers.

3. Results and discussion

Both the deeper (~1300 m) and the shallower (~850 m) intermediate depth Cd_W records, exhibit similarly low values during the LGM and document a general increase to higher values during HS1 and towards the early Holocene (Fig. 2B). The deglacial rise in Cd_W from ~0.3 nmol/kg to ~0.7 nmol/kg in the 850 m record is markedly stronger than at 1300 m, for which the increase is ~0.2 nmol/kg. While at the deeper core location Cd_W remained essentially constant since ~16 ka BP (~0.4–0.6 nmol/kg), we observe significant variations at 850 m depth. Three pronounced Cd_W maxima occur in the AAIW tongue ($> \sim 1.0$ nmol/kg) at the end of HS1 (~15.1 ka), during (~12.4–11.5 ka BP) and shortly after the YD (~11–10 ka BP), separated by lowered values during the Antarctic Cold Reversal (ACR). During the Holocene, Cd_W gradually declined from ~0.8 nmol/kg to 0.6 nmol/kg. This W-Atlantic Cd_W pattern from ~850 m water depth is in striking synchronicity with upwelling reconstructions from the SO (Anderson et al., 2009; Burke and Robinson, 2012), where AAIW is formed (Fig. 3), and suggests a close link between changes in the SO and W-Atlantic.

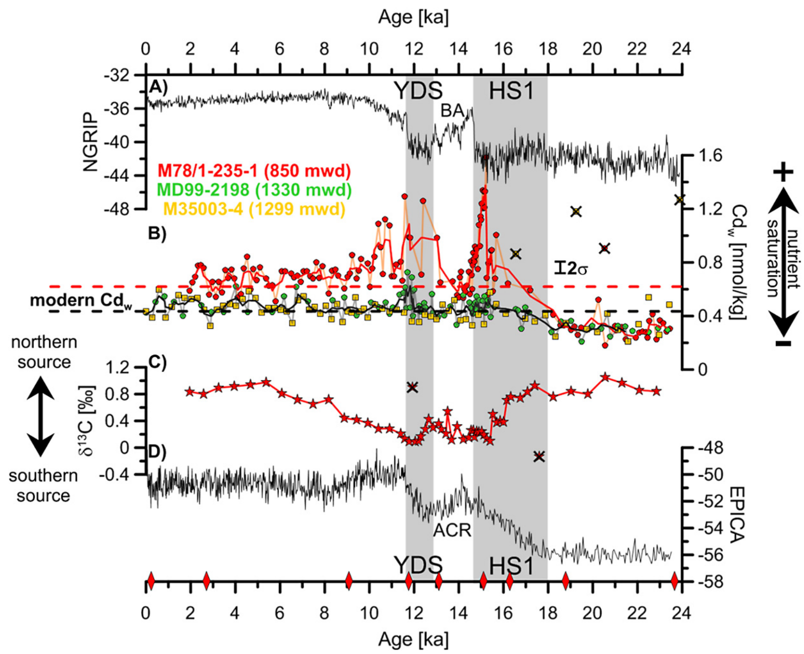

Fig. 2. Results and data treated as flyers. **A**) Oxygen isotope record of the NGRIP ice core (NGRIP Dating Group, 2006) as reference for the northern hemisphere climate signal. **B**) Cd_w of sediment core M78/1-235-1 (850 m; red, this study) and composite Cd_w record (black) from ∼1300 m (composed of sediment cores MD99-2198 (1330 m; green, this study) and M35003 (1299 m; yellow; Zahn and Stüber, 2002)) denoting nutrient saturation at intermediate water depth and beneath. Thick lines represent 3-point running averages. All Cd_w reconstructed from Cd/Ca-ratios of endobenthic species *Uvigerina spp.* Dashed lines indicate approximated modern Cd-concentrations at the appropriate depth (Mawji et al., 2015). The uncertainty based on replicate measurements is indicated (2σ). **C**) Stable carbon isotopes ($\delta^{13}C$) of core M78/1-235-1 (this study). **D**) Oxygen isotope record of the EPICA Dome C (Stenni et al., 2006) as reference for the southern hemisphere climate signal. Crossed data points were treated as flyers due to failed Grubb's test. HS1 = Heinrich Stadial 1; YD = Younger Dryas Stadial; BA = Bølling-Allerød, ACR = Antarctic Cold Reversal; Red crosses along the lower age-axis indicate ^{14}C age control points for core M78/1-235-1. (For interpretation of the references to colour in this figure legend, the reader is referred to the web version of this article.)

Northern sourced water masses are generally characterised by low nutrient concentrations and therefore by low Cd_w signatures, whereas southern sourced water masses have high nutrient concentrations and therefore high Cd_w (e.g. Came et al., 2003; Rickaby and Elderfield, 2005; Marchitto and Broecker, 2006). Hence, the general Cd_w increases at both, deep and shallow intermediate depth can either be explained by enhanced transport of AAIW to 11°N and/or the nutrient content of AAIW itself increased. The overall rise in Cd_w at ∼850 m could thus reflect a general change from a GNAIW dominated state during the LGM to an AAIW dominated state during HS1, which has persisted ever since, potentially accompanied by rapid increases of nutrient levels of AAIW itself at the end of HS1, during and shortly after the YD. The general marked increase of Cd_w from ∼0.3 to ∼0.7 nmol/kg at ∼850 m accompanied by minor changes at ∼1300 m clearly documents that the tongue of AAIW expanded northwards starting at ∼17 ka BP but was accompanied by minor changes in its vertical extent. The discrepancy between the intermediate and the deeper Cd_w-record contradicts a recent hypothesis of Meckler et al. (2013) that related enhanced opal production in the subtropical E-Atlantic during HS1 and YD to increased nutrient supply via the Atlantic-wide shoaling of Antarctic Bottom Water (AABW) even reaching intermediate water depths (Fig. 3C). An upward shift of AABW, however, cannot explain both, our shallower and deeper Cd_w-signatures. While our shallower depth Cd_w-record from 850 m water depth shows distinctive, abrupt changes in the nutrient distribution, the record from the deeper site only points to minor changes in the nutrient inventory implying that additional nutrients did not originate from below 1300 m. An Atlantic-wide upward incursion of nutrients from abyssal waters should have caused strong nutrient enrichment at the deeper site as well. Bradtmiller et al. (2016), indeed, point out that enhanced wind-driven upwelling of nutrient-rich waters took place in the E-Atlantic due to the postulated strengthening and southward shift of trade winds during times of abrupt cooling events in the northern hemisphere. Consistent with Si isotope distribution patterns from several Atlantic sediment cores (Hendry et al., 2016), increased nutrient supply via intermediate water masses feeding into the thermocline is a viable explanation for the observed opal changes in the E-Atlantic (Meckler et al., 2013).

The new data presented here may not only reveal changes in the advection but also in the nutrient content of AAIW. The low values during the LGM point to nutrient poor glacial AAIW, possibly amplified due to the admixture of GNAIW. GNAIW in fact expanded far across the equator into the southern hemisphere (Marchitto and Broecker, 2006). The increase in Cd_w during HS1 observed in both our cores thus likely reflects an overall change to higher nutrient levels of AAIW. The offset between both Cd_w records is rather related to their positions with respect to the centre of AAIW (M78/1-235-1, 850 m) and the transition zone between AAIW and northern sourced water masses below (MD99-2198, 1300 m). The latter core therefore most likely was strongly influenced by underlying northern sourced waters.

To differentiate between both the advection and the nutrient content scenarios, and to further constrain changes in water mass properties at ∼850 m in the tropical W-Atlantic, we consider the $\delta^{13}C$ signature of the epibenthic species *C. pachyderma*. The temporal pattern of $\delta^{13}C$ in the intermediate depth core M78/1-235-1 is in broad agreement with the Cd_w record (Fig. 2C). High $\delta^{13}C$ values of >0.7‰ prevailed during the LGM prior to ∼16 ka BP and during the Holocene since ∼8 ka BP. Distinct $\delta^{13}C$ minima of ∼0–0.2‰ occurred during the end of HS1 and during the YD, synchronous with the Cd_w maxima, interrupted by elevated values during the ACR. These $\delta^{13}C$ minima are a common feature of (sub)tropical intermediate depth $\delta^{13}C$ reconstructions (e.g. Curry and Oppo, 2005; Romahn et al., 2014) and are considered to reflect upwelling

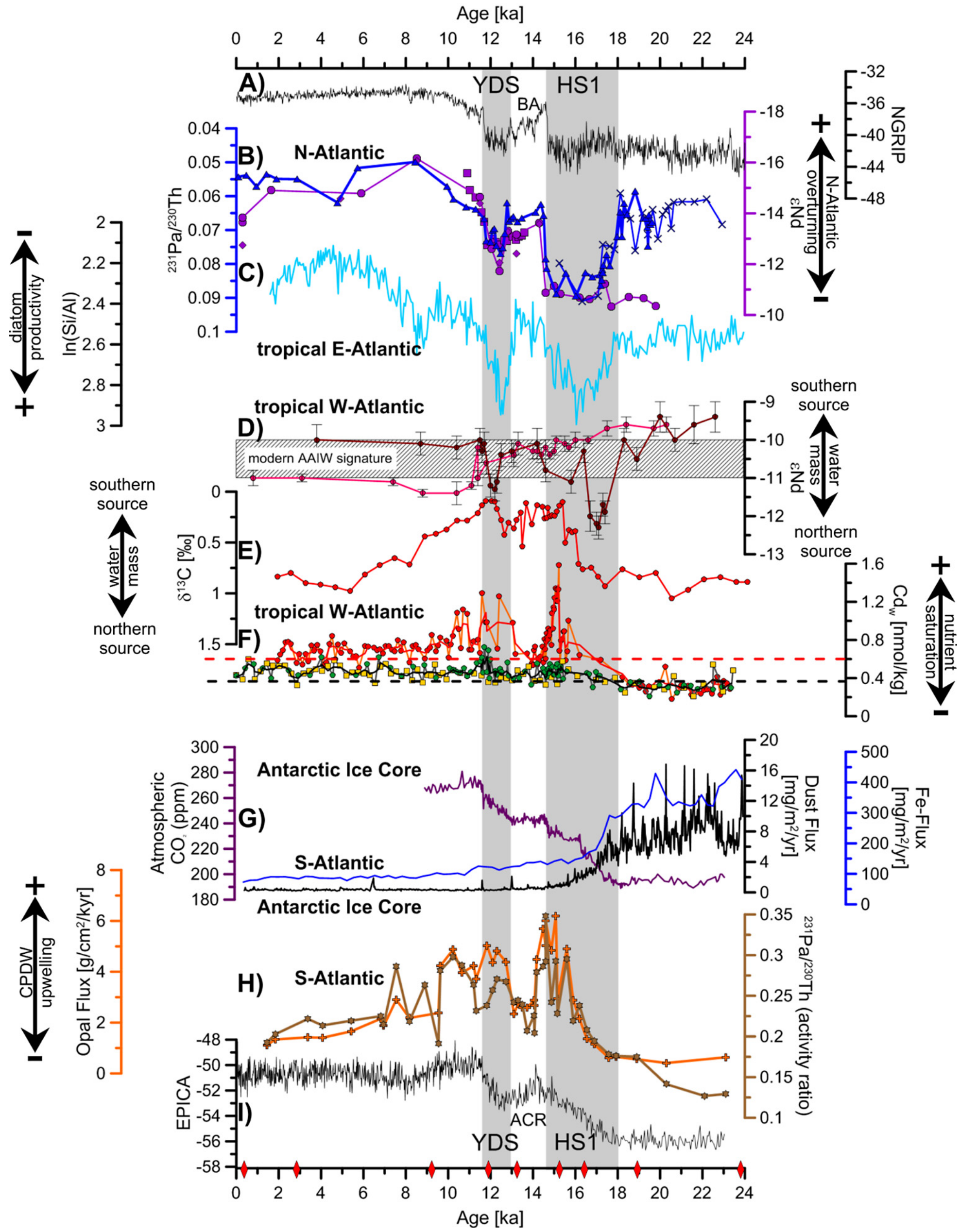

Fig. 3. Intermediate water mass evolution of the tropical E- and W-Atlantic compared to N- and S-Atlantic circulation records for the last glacial termination. **A**) Oxygen isotope record of the Greenland NGRIP ice core (NGRIP Dating Group, 2006) as reference reflecting the northern hemisphere climate signal. **B**) Pa/Th (blue) and εNd (purple) records of N-Atlantic sediment core ODP Site 1063 (Böhm et al., 2015 and references therein) indicating N-Atlantic overturning strength. **C**) Ln(Si/Al) (light blue) of tropical E-Atlantic sediment core ODP Site 658 (Meckler et al., 2013) showing changes in diatom productivity. **D**) εNd reconstructions from the Bonaire Basin (pink, Xie et al., 2014, 1079 m) and the Demarara Rise, off Brazil (brown, Huang et al., 2014, 947 m). Shaded area indicates modern εNd signature of AAIW in the tropical W-Atlantic (Osborne et al., 2014). **E**) Stable carbon isotopes (δ^{13}C, red) of core M78/1-235-1 (this study). **F**) Cd_w of sediment core M78/1-235-1 (850 m; red, this study) and composite Cd_w record (black) from ~1300 m (composed of sediment cores MD99-2198 (1330 m; green, this study) and M35003 (1299 m; yellow, Zahn and Stüber, 2002)) denoting nutrient saturation at intermediate water depth. Thick lines represent 3-point running averages. All Cd_w reconstructed from Cd/Ca-ratios of endobenthic species *Uvigerina spp.* Dashed lines indicate approximated modern Cd-concentrations at the appropriate depth (Mawji et al., 2015). **G**) Atmospheric CO_2 evolution, reconstructed from Antarctic ice core analyses (purple, Marcott et al., 2014), dust flux (black, Lambert et al., 2012) and Fe flux in the SO (blue, Martínez-García et al., 2011). **H**) Opal flux (orange) and Pa/Th (brown) records of S-Atlantic sediment core TN057-13 showing upwelling changes of nutrient-rich CPDW (Anderson et al., 2009). **I**) Oxygen isotope record of the Antarctica EPICA Dome C (Stenni et al., 2006) as reference reflecting the southern hemisphere climate signal. HS1 = Heinrich Stadial 1; YD = Younger Dryas Stadial; BA = Bølling-Allerød; ACR = Antarctic Cold Reversal; Red diamonds along the lower age-axis indicate ^{14}C age control points for core M78/1-235-1. (For interpretation of the references to colour in this figure legend, the reader is referred to the web version of this article.)

of deep, old and δ^{13}C depleted Circumpolar Deepwater (CPDW) in the SO, of which the isotope signal was then transferred to low latitudes such as our intermediate depth core location via AAIW (e.g. Pena et al., 2013). The contribution of GNAIW with its significantly heavier δ^{13}C signature of 1.5‰ (Curry and Oppo, 2005) can therefore be ruled out at the depth of our core location. Thornalley et al. (2010) observed similar negative excursions in the northern N-Atlantic and interpreted these as a shift from southern sourced waters mixing with GNAIW to southern sourced waters mixing with northern high latitude brine waters. This mechanism is unlikely to have caused the HS1 and YD δ^{13}C signatures presented here. The regional setting differs significantly from the one in the northern N-Atlantic (Fig. 1) as the northern sourced water masses in the intermediate tropical W-Atlantic

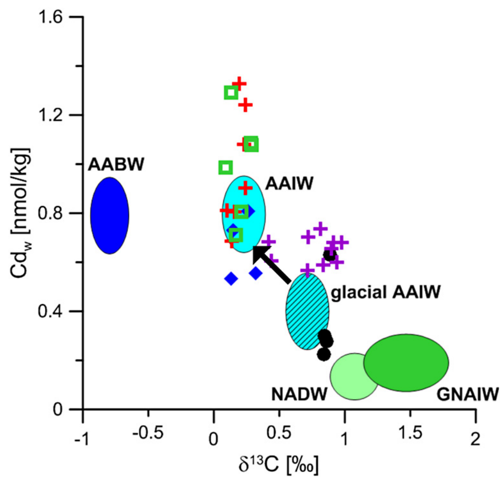

Fig. 4. Evolution of intermediate water depth nutrient levels as reflected by combined Cd_w and $\delta^{13}C$ signatures. Modern and suggested glacial water mass signatures indicated by ellipses (Curry and Oppo, 2005; Marchitto and Broecker, 2006; Mawji et al., 2015). Time series data separated for distinct time intervals: black dots = Last Glacial Maximum; red crosses = Heinrich Stadial 1; open green squares = Younger Dryas Stadial; blue diamonds = Bølling-Allerød; purple crosses = Holocene; AABW = Antarctic Bottom Water; AAIW = Antarctic Intermediate Water; NADW = North Atlantic Deep Water; GNAIW = Glacial North Atlantic Intermediate Water; Black arrow indicates postulated shift in AAIW signature. (For interpretation of the references to colour in this figure legend, the reader is referred to the web version of this article.)

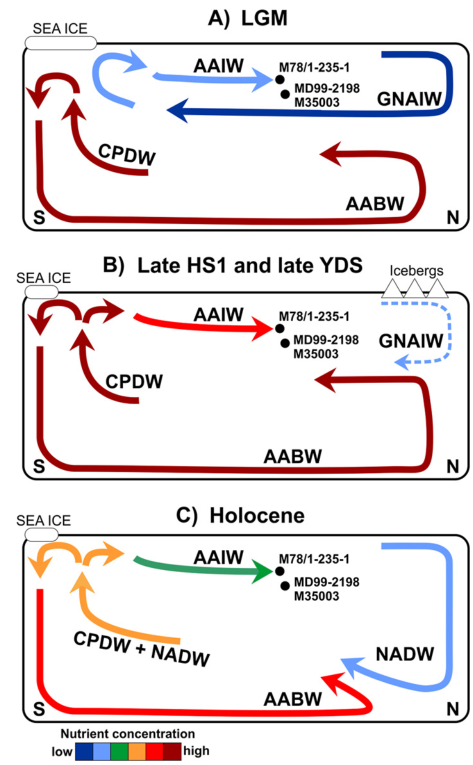

Fig. 5. Schematic illustration of different Atlantic overturning modes complemented from the Cd_w and $\delta^{13}C$ reconstructions (following Talley, 2013 and Ferrari et al., 2014). Water masses and flow are indicated by arrows. Colour-coding implies nutrient concentrations (see legend). Locations of proxy records from this study are indicated by black dots. **A**) Last Glacial Maximum: The AMOC is characterised by clearly separated overturning cells. In the shallow cell, AAIW is mainly fed by nutrient depleted, shallow GNAIW resulting in low Cd_w and high $\delta^{13}C$ signatures at intermediate depths in the tropical W-Atlantic. As Antarctic sea ice cover is largely expanded, upwelling of nutrient-rich CPDW and according air–sea-exchange is hampered. CPDW sinks to the abyss and forms AABW in the deep cell. **B**) Late Heinrich Stadial 1 and shortly after the Younger Dryas Stadial: Due to warming in the southern hemisphere large scale Antarctic sea-ice retreated fostered the shallow upwelling of CPDW north of the ice edge, feeding both AABW and AAIW. The formation of GNAIW in contrast was suppressed. AAIW therefore was characterised by high nutrient conditions and low $\delta^{13}C$, as reflected by the new data. **C**) Holocene: The modern AMOC is characterised by the strengthened formation of oxygenated NADW, ventilating the deep Atlantic. Modern AAIW is thereby fed by a mixture of CPDW and NADW, causing mediocre benthic Cd_w. Relatively positive benthic $\delta^{13}C$ values imply a considerable contribution from northern sources.

are characterised by high $\delta^{13}C$ signatures (Curry and Oppo, 2005; Marchitto and Broecker, 2006). The intermediate depth $\delta^{13}C$ minima observed here more likely originated from subantarctic surface waters, where AAIW is formed (e.g. Spero and Lea, 2002; Romahn et al., 2014). The change in $\delta^{13}C$ observed at our location therefore points to a shift in the AAIW source waters from GNAIW during the LGM to CPDW at the end of HS1 and during the YD.

The Cd_W and $\delta^{13}C$ reconstructions presented here allow the contrasting views on the northward advection of AAIW during the YD and HS1 to be reconciled. Our data imply that AAIW continuously reached the tropical W-Atlantic during the last 24 ka although its nutrient composition and $\delta^{13}C$ signature varied significantly as a consequence of SO circulation changes (Figs. 3, 4).

The prevalence of GNAIW or CPDW sourced AAIW is also consistent with nearby foraminifera/fish debris Nd isotope data from intermediate water depths (Fig. 3D; Huang et al., 2014 (KNR197-3-46CDH from 947 m); Xie et al., 2014 (VM12-107 from 1079 m)). These two intermediate depth ε Nd records conflict in detail but the data mostly fall within the range of -10 to -11εNd typical for modern AAIW in the tropical W-Atlantic (Huang et al., 2014; Osborne et al., 2014). Therefore, although the decrease in εNd from a GNAIW like signature of -9.7 (Gutjahr et al., 2008) in the LGM to -11.4 in the early Holocene can be explained by a change from GNAIW to NADW (Xie et al., 2014), these changes could also be explained by variability of εNd within AAIW. A change in the εNd signature of AAIW is consistent with a change of source waters feeding AAIW. With GNAIW as the main source for AAIW during the LGM and a combination of NADW and CPDW today as suggested from proxy data and modelling by Talley (2013) and Ferrari et al. (2014), this change in source waters would have altered the AAIW εNd signature accordingly. The offsets between the two εNd records (Huang et al., 2014; Xie et al., 2014) are likely the result of their different locations within different parts of the AAIW tongue. Furthermore exchange processes with the sediments may have caused sharp excursions to unradiogenic εNd values given that the detrital sediments in the region have values of ~ -13 (Weiss et al., 1985; Howe et al., 2016). Recently published data from the Brazil Margin further confirmed suggestions of Xie et al. (2014) that the reliability of different techniques to extract the seawater εNd near ocean margins needs to be tested and confirmed for each location (Howe et al., 2016). Sedimentary exchange process may thus be an important cause of the divergence of εNd time series from the W-Atlantic (Pahnke et al., 2008; Xie et al., 2012, 2014; Huang et al., 2014).

The timing of our Cd_W and $\delta^{13}C$ excursions at the end of HS1 and YD and the comparison of the records from ~850 m depth to Pa/Th and Nd isotope data from the deep N-Atlantic (Fig. 3B; Böhm et al., 2015) and to biogenic opal flux and Pa/Th data from the SO (Fig. 3H; Anderson et al., 2009) supports SO upwelling changes as the main driver of the nutrient content of low latitude AAIW.

It has been hypothesised that during the LGM, the Atlantic circulation was separated into two overturning cells (Ferrari et al., 2014). A shallow cell was driven by the formation of relatively shallow GNAIW in the N-Atlantic, which flowed southwards and fed glacial AAIW in the S-Atlantic given that the nutrient-rich CPDW did not upwell to the surface where AAIW is formed, at that time. The deep cell instead, was characterised by northward flowing AABW, which filled the Atlantic basin at depth and recirculated at shallower depths (e.g. Sigman et al., 2010; Ferrari et al., 2014). Due to the extended Antarctic sea ice cover, the deep overturning cell was isolated from the atmosphere and therefore carbon and nutrients were stored in the abyss (e.g. Stephens and Keeling, 2000; Gersonde et al., 2005) (Fig. 5A). A distinct boundary between both cells (e.g. Marchitto and Broecker, 2006; Lund et al., 2015) and a modified distribution of deep water properties likely prevailed (e.g. Lynch-Stieglitz et al., 2007). The modern overturning circulation in contrast, is controlled by the formation of NADW in the N-Atlantic, which flows southwards, mixes with CPDW and both contribute to the formation of AAIW in the SO (Talley, 2013) (Fig. 5C).

For the last deglaciation, we propose a circulation pattern deviating from the above-mentioned overturning cells. The southern hemisphere experienced two warmer periods during the deglaciation separated by the ACR (e.g. Blunier et al., 1997; Stenni et al., 2006; Denton et al., 2010) (Fig. 3I). These warm intervals coincided with the HS1 and the YD intervals, during which the northern hemisphere experienced abrupt cooling and a weakening or even a collapse of the AMOC (Fig. 3B; McManus et al., 2004; Böhm et al., 2015). The corresponding slowdown of northward heat transport led to the warming of the southern hemisphere (Crowley, 1992; Toggweiler and Lea, 2010) and consequently the westerly wind belt shifted southward (e.g. Denton et al., 2010). Anderson et al. (2009) suggested that the shift of the Westerlies caused a strengthening of the upwelling of nutrient-rich CPDW leading to higher productivity (Fig. 3H) and CO_2 release in the SO during HS1 and YD (e.g. Burke and Robinson, 2012; Jaccard et al., 2016). These mechanisms are likely to have been augmented by changes in the role of northern component waters and their southward expansion for the deglacial CO_2 rise (e.g. Hain et al., 2014; Chen et al., 2015; Lund et al., 2015).

The striking synchronicity of our 850 m intermediate depth Cd_W and $\delta^{13}C$ records to S-Atlantic biogenic opal flux supports the notion that upwelling CPDW has driven the nutrient inventory of AAIW on deglacial millennial timescales.

We argue that the deglacial change in nutrient inventory at intermediate depths reflects the varying admixture of sources to AAIW and hence, provides evidence for the reconnection of the shallow and the deep Atlantic overturning cells (Figs. 4 and 5). During the LGM, when both overturning cells were separated from each other, the contribution of low nutrient GNAIW to AAIW formation (Ferrari et al., 2014) is evident in low Cd_W values at ~850 m in the tropical W-Atlantic. In contrast, the Cd_W maxima at the end of HS1, during and shortly after the YD suggest a complete cessation of GNAIW contributions in favour of high nutrient CPDW, feeding SO productivity and AAIW (Fig. 5B). The sharp drop in Cd_W at the beginning of the BA may indicate a link to a postulated short-term “overshooting event“ characterised by enhanced AMOC strength that lasted only a few hundreds of years (Chen et al., 2015). There is evidence, that the YD climatic rebound was necessary to complete the last termination by raising atmospheric CO_2, which fostered interglacial warm conditions (Denton et al., 2010). During the post YD warming, the Atlantic overturning strengthened and deepened to its modern state (Ferrari et al., 2014). A second postulated short-term AMOC strengthening event (Chen et al., 2015) may have caused the distinct negative Cd_W excursion at the beginning of the Holocene. The ultimate Holocene reconnection of both overturning cells is consistent with our intermediate depth Cd_W values documenting modern contributions of both, nutrient-rich CPDW and nutrient depleted NADW. Today, nutrient levels at intermediate water depths in the equatorial W-Atlantic are higher than during the LGM, but significantly lower than at times when AAIW did not receive any NADW contribution (during late HS1, during and shortly after the YD).

Our study suggests that the tropical W-Atlantic nutrient inventory of AAIW was mainly controlled by SO sea ice extent, upwelling of deeper water masses in the SO and related atmospheric processes rather than by deep water formation processes in the N-Atlantic. Of particular importance for the nutrient levels of AAIW, were periods of intense upwelling of CPDW in the SO causing pronounced increases in primary productivity during HS1 and the YD (Anderson et al., 2009). We speculate that during deglacial periods of prevailing increased Cd_W, the complete utilisation of nutrients in the “high-nutrient, low-chlorophyll” SO was hampered by low iron fluxes and the lack of metabolizable iron (e.g. Lambert et al., 2012; Martínez-García et al., 2011, 2014). The reduced nutrient utilisation in the SO would have allowed a large portion of unused nutrients to be transported northward via AAIW causing prominent intermediate-depth Cd_W maxima in the tropical W-Atlantic.

Increased low and high latitude Atlantic primary productivity, fostered by the nutrient injection via AAIW, likely enhanced the biological pump and thus is a possible cause of the deglacial atmosphere CO_2 plateau at the end of HS1 (Marcott et al., 2014) (Fig. 3G). Increased diatom productivity during HS1 in the N-Atlantic may reflect the high nutrient supply during this time (Gil et al., 2010; Hendry et al., 2016). Enhanced silicic acid supply to the NE-Atlantic during northern hemisphere cooling events further implies a weakened stratification (Hendry et al., 2016). Further support for the postulated short-term AAIW fertilisation by old nutrient-rich deep waters and the subsequent transfer to the tropical W-Atlantic comes from cold water coral $\Delta^{14}C$ off Brazil and in the western N-Atlantic, pointing to higher ventilation ages and thus, the presence of southern sourced waters during HS1 and YD (Robinson et al., 2005; Mangini et al., 2010). Proxy data from the Drake Passage indicate that the Southern Ocean ventilation increased during these times (Burke and Robinson, 2012), which through AAIW, had far reaching effects on the biological pump globally.

4. Conclusions

High resolution reconstructions of intermediate water Cd_W concentrations and $\delta^{13}C$ suggest that AAIW continuously reached the tropical N-Atlantic during the entire last 24 ka and underwent only minor shifts in northward expansion. At the end of HS1, as well as during and shortly after the YD the AAIW was enriched in Cd_W indicating a change of source water masses feeding AAIW from low nutrient GNAIW to high nutrient CPDW. The striking resemblance of our Cd_W reconstructions from ~850 m depth to upwelling reconstructions from the Atlantic sector of the SO and postulated short-term AMOC strengthening during the BA and at the beginning of the Holocene demonstrate that the SO effectively shaped the N-Atlantic nutrient inventory. In contrast, our Cd_W results from nearby but deeper intermediate water depth location (~1300 m) preclude a recent theory arguing for Atlantic wide shoaling of AABW. The increased AAIW nutrient content at intermediate depth likely enhanced N-Atlantic productivity and hence led to a dampening of the deglacial global atmospheric CO_2 increase. The new AAIW Cd_W and $\delta^{13}C$ data demonstrate the importance of deglacial ocean circulation reorganisations for global marine biogeochemistry and climate.

Acknowledgements

This research was funded by the Deutsche Forschungsgemeinschaft (DFG) via the “Cluster of Excellence – The Future Ocean” Kiel; Project number CP1142. We are thankful for the detailed and constructive comments of two anonymous reviewers which substantially improved this manuscript.

Appendix A. Online content

Cd_W and $\delta^{13}C$ data are available online at the Data Publisher for Earth and Environmental Science, PANGEA: www.pangea.de.

Supporting information associated with this article can be found in the online version at http://dx.doi.org/10.1016/j.epsl.2017.01.030.

References

Anderson, R.F., et al., 2009. Wind-driven upwelling in the Southern ocean and the deglacial rise in atmospheric CO_2. Science 323 (5920), 1443–1448.
Blunier, T., et al., 1997. Timing of the Antarctic Cold Reversal and the atmospheric CO_2 increase with respect to the Younger Dryas event. Geophys. Res. Lett. 24 (21), 2683–2686.
Böhm, E., et al., 2015. Strong and deep Atlantic meridional overturning circulation during the last glacial cycle. Nature 517 (7532), 73–76.
Boyer, T.P., et al., 2013. World Ocean Database 2013. In: Levitus, S., Mishonov, A. (Eds.), NOAA Atlas NESDIS 72. Silver Spring, MD. 209 pp. http://doi.org/10.7289/V5NZ85MT.
Boyle, E.A., 1988. Cadmium: chemical tracer of deepwater paleoceanography. Paleoceanography 3 (4), 471–489.
Boyle, E.A., 1992. Cadmium and $\delta^{13}C$ paleochemical ocean distributions during the stage 2 glacial maximum. Annu. Rev. Earth Planet. Sci. Lett. 20, 245–287.
Boyle, E.A., Rosenthal, Y., 1996. Chemical hydrography of the South Atlantic during the last glacial maximum: Cd vs. $\delta^{13}C$. In: The South Atlantic. Springer, Berlin, Heidelberg, pp. 423–443.
Bradtmiller, L.I., et al., 2016. Changes in biological productivity along the northwest African margin over the past 20,000 years. Paleoceanography 31 (1), 185–202.
Broecker, W.S., 1998. Paleocean circulation during the Last Deglaciation: a bipolar seesaw? Paleoceanography 13 (2), 119–121.
Bryan, S.P., Marchitto, T.M., 2010. Testing the utility of paleonutrient proxies Cd/Ca and Zn/Ca in benthic foraminifera from thermocline waters. Geochem. Geophys. Geosyst. 11 (1).
Burke, A., Robinson, L.F., 2012. The Southern Ocean's role in carbon exchange during the last deglaciation. Science 335 (6068), 557–561.
Came, R.E., Oppo, D.W., Curry, W.B., 2003. Atlantic Ocean circulation during the Younger Dryas: insights from a new Cd/Ca record from the western subtropical South Atlantic. Paleoceanography 18 (4).
Came, R.E., et al., 2008. Deglacial variability in the surface return flow of the Atlantic meridional overturning circulation. Paleoceanography 23 (1).
Chen, T., et al., 2015. Synchronous centennial abrupt events in the ocean and atmosphere during the last deglaciation. Science 349 (6255), 1537–1541.
Crowley, T.J., 1992. North Atlantic deep water cools the southern hemisphere. Paleoceanography 7 (4), 489–497.
Curry, W.B., Oppo, D.W., 2005. Glacial water mass geometry and the distribution of $\delta^{13}C$ of ΣCO_2 in the western Atlantic Ocean. Paleoceanography 20, PA1017. http://dx.doi.org/10.1029/2004PA001021.
Denton, G.H., et al., 2010. The last glacial termination. Science 328 (5986), 1652–1656. http://dx.doi.org/10.1126/science.1184119.
Duplessy, J.-C., et al., 1984. ^{13}C record of benthic foraminifera in the last interglacial ocean: implications for the carbon cycle and the global deep water circulation. Quat. Res. 21 (2), 225–243.
Ferrari, R., et al., 2014. Antarctic sea ice control on ocean circulation in present and glacial climates. Proc. Natl. Acad. Sci. USA 111 (24), 8753–8758. http://dx.doi.org/10.1073/pnas.1323922111.
Gersonde, R., et al., 2005. Sea-surface temperature and sea ice distribution of the Southern Ocean at the EPILOG Last Glacial Maximum—a circum-Antarctic view based on siliceous microfossil records. Quat. Sci. Rev. 24 (7), 869–896.
Gherardi, et al., 2009. Glacial–interglacial circulation changes inferred from $^{231}Pa/^{230}Th$ sedimentary record in the North Atlantic region. Paleoceanography 24, PA2204. http://dx.doi.org/10.1029/2008PA001696.
Gil, I.M., Keigwin, L.D., Abrantes, F., 2010. Comparison of diatom records of the Heinrich Event 1 in the Western North Atlantic. IOP Conf. Ser.: Earth Environ. Sci. http://dx.doi.org/10.1088/1755-1315/9/1/012008.
Greaves, M., et al., 2008. Interlaboratory comparison study of calibration standards for foraminiferal Mg/Ca thermometry. Geochem. Geophys. Geosyst. 9 (8).
Gutjahr, M., et al., 2008. Tracing the Nd isotope evolution of North Atlantic deep and intermediate waters in the Western North Atlantic since the Last Glacial Maximum from Blake Ridge sediments. Earth Planet. Sci. Lett. 266 (1), 61–77.
Hain, M.P., Sigman, D.M., Haug, G.H., 2014. Distinct roles of the Southern Ocean and North Atlantic in the deglacial atmospheric radiocarbon decline. Earth Planet. Sci. Lett. 394, 198–208.
Hathorne, E.C., et al., 2012. Online preconcentration ICP-MS analysis of rare earth elements in seawater. Geochem. Geophys. Geosyst. 13 (1), Q01020. http://dx.doi.org/10.1029/2011GC003907.
Hendry, K.R., et al., 2012. Abrupt changes in high-latitude nutrient supply to the Atlantic during the last glacial cycle. Geology 40 (2), 123–126.
Hendry, K.R., et al., 2016. Deglacial diatom production in the tropical North Atlantic driven by enhanced silicic acid supply. Earth Planet. Sci. Lett. 438, 122–129.
Hoffmann, J., et al., 2014. Disentangling abrupt deglacial hydrological changes in northern South America: insolation versus oceanic forcing. Geology 42 (7), 579–582.
Howe, J.N.W., et al., 2016. Antarctic intermediate water circulation in the South Atlantic over the past 25,000 years. Paleoceanography 31, 1302–1314.
Huang, K.-F., Oppo, D.W., Curry, W.B., 2014. Decreased influence of Antarctic intermediate water in the tropical Atlantic during North Atlantic cold events. Earth Planet. Sci. Lett. 389, 200–208.
Jaccard, S.L., et al., 2016. Covariation of deep Southern Ocean oxygenation and atmospheric CO_2 through the last ice age. Nature 530, 207–210.
Lambert, F., et al., 2012. Centennial mineral dust variability in high-resolution ice core data from Dome C, Antarctica. Clim. Past 8 (2), 609–623.
Lund, D.C., et al., 2015. Southwest Atlantic water mass evolution during the last deglaciation. Paleoceanography 30, 477–494.
Lynch-Stieglitz, J., et al., 2007. Atlantic meridional overturning circulation during the last glacial maximum. Science 316, 66–69.
Mangini, A., et al., 2010. Deep sea corals off Brazil verify a poorly ventilated Southern Pacific Ocean during H2, H1 and the Younger Dryas. Earth Planet. Sci. Lett. 293 (3–4), 269–276.
Marchitto, T.M., Broecker, W.S., 2006. Deep water mass geometry in the glacial Atlantic Ocean: a review of constraints from the paleonutrient proxy Cd/Ca. Geochem. Geophys. Geosyst. 7 (12).
Marcott, S.A., et al., 2014. Centennial-scale changes in the global carbon cycle during the last deglaciation. Nature 514 (7524), 616–619.
Martínez-García, A., et al., 2011. Southern Ocean dust-climate coupling over the past four million years. Nature 476 (7360), 312–315.
Martínez-García, A., et al., 2014. Iron fertilization of the Subantarctic Ocean during the last ice age. Science 343 (6177), 1347–1350.
Mawji, E., et al., 2015. The GEOTRACES Intermediate Data Product 2014. Mar. Chem. http://dx.doi.org/10.1016/j.marchem.2015.04.005.
McManus, J.F., et al., 2004. Collapse and rapid resumption of Atlantic meridional circulation linked to deglacial climate changes. Nature 428 (6985), 834–837.
Meckler, A.N., et al., 2013. Deglacial pulses of deep-ocean silicate into the subtropical North Atlantic Ocean. Nature 495 (7442), 495–498.
NGRIP Dating Group, 2006. Greenland Ice Core Chronology 2005, (GICC05). IGBP PAGES/World Data Center for Paleoclimatology. Data Contribution Series # 2006-118. NOAA/NCDC Paleoclimatology Program, Boulder CO, USA.
Osborne, A.H., et al., 2014. Neodymium isotopes and concentrations in Caribbean seawater: tracing water mass mixing and continental input in a semi-enclosed ocean basin. Earth Planet. Sci. Lett. 406, 174–186.
Pahnke, K., Goldstein, S.L., Hemming, S.R., 2008. Abrupt changes in Antarctic Intermediate Water circulation over the past 25,000 years. Nat. Geosci. 1 (12), 870–874.
Pena, L., et al., 2013. Rapid changes in meridional advection of Southern Ocean intermediate waters to the tropical Pacific during the last 30 kyr. Earth Planet. Sci. Lett. 368, 20–32.
Reimer, P.J., et al., 2013. IntCal13 and Marine13 radiocarbon age calibration curves 0–50,000 years cal BP. Radiocarbon 55 (4).
Rickaby, R.E.M., Elderfield, H., 2005. Evidence from the high-latitude North Atlantic for variations in Antarctic Intermediate water flow during the last deglaciation. Geochem. Geophys. Geosyst. 6 (5).
Robinson, L.F., et al., 2005. Radiocarbon variability in the western North Atlantic during the last deglaciation. Science 310 (5753), 1469–1473.
Romahn, S., Mackensen, A., Groeneveld, J., 2014. Deglacial intermediate water reorganization: new evidence from the Indian Ocean. Clim. Past 10 (1), 293–303.
Rosenthal, Y., Boyle, E., Labeyrie, L., 1997. Last glacial maximum paleochemistry and deepwater circulation in the Southern Ocean: evidence from foraminiferal cadmium. Paleoceanography 12 (6), 787–796.
Schlitzer, R., 2015. Ocean Data View. http://odv.awi.de.
Sigman, D.M., Hain, M.P., Haug, G.H., 2010. The polar ocean and glacial cycles in atmospheric CO_2 concentration. Nature 466, 47–55.
Spero, H.J., Lea, D.W., 2002. The cause of carbon isotope minimum events on glacial terminations. Science 296 (5567), 522–525.
Stenni, B., et al., 2006. EPICA Dome C Stable Isotope Data to 44.8 KYr BP. IGBP PAGES/World Data Center for Paleoclimatology Data Contribution Series # 2006-112. NOAA/NCDC Paleoclimatology Program, Boulder CO, USA.
Stephens, B.B., Keeling, R.F., 2000. The influence of Antarctic sea ice on glacial–interglacial CO_2 variations. Nature 404 (6774), 171–174.
Talley, L.D., 2013. Closure of the global overturning circulation through the Indian, Pacific, and Southern Oceans: schematics and transports. Oceanography 26 (1), 80–97. http://dx.doi.org/10.5670/oceanog.2013.07.
Thornalley, D.J.R., Elderfield, H., McCave, I.N., 2010. Intermediate and deep water paleoceanography of the northern North Atlantic over the past 21,000 years. Paleoceanography 25 (1).
Toggweiler, J.R., Lea, D.W., 2010. Temperature differences between the hemispheres and ice age climate variability. Paleoceanography 25, PA2212. http://dx.doi.org/10.1029/2009PA001758.

Weiss, R.F., et al., 1985. Atmospheric chlorofluoromethanes in the deep equatorial Atlantic. Nature 314, 608–610.

Xie, R.C., Marcantonio, F., Schmidt, M.W., 2012. Deglacial variability of Antarctic Intermediate Water penetration into the North Atlantic from authigenic neodymium isotope ratios. Paleoceanography 27, PA3221.

Xie, R.C., Marcantonio, F., Schmidt, M.W., 2014. Reconstruction of intermediate water circulation in the tropical North Atlantic during the past 22,000 years. Geochim. Cosmochim. Acta 140 (0), 455–467.

Zahn, R., Stüber, A., 2002. Suborbital intermediate water variability inferred from paired benthic foraminiferal Cd/Ca and δ^{13}C in the tropical West Atlantic and linking with North Atlantic climates. Earth Planet. Sci. Lett. 200, 191–205.

Zahn, R., Winn, K., Sarthein, M., 1986. Benthic foraminiferal δ^{13}C and accumulation rates of organic carbon: Uvigerina peregrina group and Cibicidoides wuellerstorfi. Paleoceanography 1, 27–42.